ASIA TURBOMACHINERY & PUMP SYMPOSIUM
23-26 FEBRUARY 2021
SHORT COURSES: 22 FEBRUARY 2021

DEVELOPMENT AND APPLICATION OF VERY HIGH FLOW COVERED STAGES FOR PROCESS CENTRIFUGAL COMPRESSORS

Vishal Jariwala
Aerodynamics Engineer
R&D Aero and Structural Dynamics
Elliott Group
Jeannette, PA, USA

Rambabu Chundru
Solid Mechanics Engineer
R&D Aero and Structural Dynamics
Elliott Group
Jeannette, PA, USA

Brian Pettinato
Manager
R&D Aero & Structural Dynamics
Elliott Group
Jeannette, PA, USA

Vishal Jariwala is an Aerodynamics Engineer in Research and Development at Elliott Group, Jeannette, PA. He designs centrifugal compressor stages using analytical methods including computational fluid dynamics (CFD). His experience also includes centrifugal compressor prototype testing, CFD algorithm development, and software development. He is interested in all things related to aerodynamics as well as novel applications of sensors. He holds a Master's degree in Aerospace Engineering from The University of Michigan – Ann Arbor, and a Bachelor's in Mechanical Engineering from Regional Engineering College, Surat, India. In Pennsylvania, he has obtained Engineering-in-Training (EIT) certification. He is also a member of ASME IGTI's Turbomachinery Committee. Vishal is an avid radio-controlled aircraft flyer and a General-class amateur radio operator.

Rambabu Chundru is a Mechanical Engineer at Elliott Group in Jeannette, Pennsylvania. He has been with Elliott Group since 2010. His area of expertise is turbomachinery design including Finite Element Analysis and modal testing. He currently manages Solid Mechanics group. He received his B.S. in Mechanical Engineering from Nagarjuna University, India in 1999 and M.S. in Engineering Design from Bharathiar University in 2001 and MBA from University of Pittsburgh in 2017. Prior to joining Elliott Group, he worked as a Mechanical Engineer at Pratt & Whitney and Hamilton Sundstrand.

Brian Pettinato is Manager of the R&D Aero and Structural Dynamics Department at Elliott Group in Jeannette, Pennsylvania. He has been with Elliott Group since 1995. His primary area of expertise is machinery dynamics. Prior to joining Elliott Group, he worked as a project engineer for CentriMarc. Mr. Pettinato received his B.S. (1989) and M.S. (1992) Mechanical Engineering degrees from the University of Virginia. He has coauthored over twenty technical papers and holds three U.S. patents. Mr. Pettinato is a fellow member of ASME, a member of STLE, and a registered Professional Engineer in the State of Pennsylvania. He serves on the Turbomachinery Advisory Committee of Texas A&M and on the API 684 rotor dynamics task force.

ABSTRACT

For process centrifugal compressor applications, achieving higher flow rates through a given sized compressor can reduce capital cost while still meeting process requirements. Key technologies for enabling such higher flow rates are high flow coefficient (design $\phi > 0.12$) and very high flow coefficient (design $\phi > 0.20$) aerodynamic staging featuring covered impellers. Since the 1990s the prevalence of high flow coefficient stages has only increased in LNG, Ethylene, and some other compression services. The overall trend has been towards higher flow coefficient stages that push beyond existing experience limits. Applications involving what can be termed as very high flow (VHF) coefficient staging have only first been applied since around 2010. The present work describes the development and application of a family of very high flow (VHF) stages with nominal design flow coefficient of 0.24 and moderate to high Machine Mach Number (Mu) of 0.88. The design is essentially a constrained optimization where the stage aerodynamic performance (range and efficiency) is optimized while still meeting targets related to mechanical robustness and rotor dynamic usability.

The first part of the paper describes the aerodynamic design focusing on the features that help address the aerodynamic performance requirements. As the design flow coefficient increases, both the efficiency and the available stable operating range become further challenged, especially as the inlet relative Mach number increases. The presented aerodynamic stage design solution consists of an impeller with both full and splitter blades having unique features and a return channel system that also features three-dimensional blading, which extends into the cross-over section.

Subsequent parts of the paper discuss the mechanical design, single stage aerodynamic rig testing, selection examples, and a case study involving results from a tested shop order.

INTRODUCTION

Process centrifugal compressors are critical components in chemical production processes. With the increase in plant throughput, the volumetric flow handled by these compressors must scale up too. One obvious solution is the corresponding scaling up of the compressor casing and internals based on existing technology. This has been done in the past (Turbo. Intl., 2009) up to the "mega" scale, but it is not always viable due to the disproportionate increase in capital cost when equipment reaches beyond a certain size. This jump in capital and maintenance cost is driven by such factors as methods of manufacture, material availability, logistics and general increased difficulty handling extremely large and heavy equipment (Josefczyk and Jones, 2018). A better solution can be provided by developing staging and technology that enables the passing of higher volumetric flow in a given frame size (Harvey, 2019). Such high flow capacity stages allow for a smaller compressor frame with an additional benefit of higher operating speed, which is typically a better match for a steam turbine driver. The cumulative effect is one of reduced CAPEX and life-cycle costs.

Centrifugal stages with small bore as well as uncovered impellers are common in the very high flow coefficient range. However, stages with covered impellers with relatively large impeller bore diameters as applied in multistage applications are not prevalent in the very high flow coefficient range. Among other challenges to designing such stages, the additional mass of the impeller cover causes significant structural issues and limits the design options for impeller blades.

As discussed by Aungier (2000), a high design flow coefficient generally place a radial compressor into a sub-optimal performance zone where both the efficiency and the available, stable operating range suffer, especially as the Inlet Relative Mach Number (Ma) increases. Casey (2010) discusses impeller architecture as a function of specific speed. Corbo (2018) outlines the redesign effort for a high flow centrifugal stage having a flow coefficient of 0.16. The current work presented herein goes a step further by pushing the design for a covered inline centrifugal stage out to an even higher flow coefficient of 0.24, which presents new aerodynamic and mechanical performance challenges.

VERY HIGH FLOW COEFFICIENT (VHF) PROCESS CENTRIFUGAL STAGE DESIGN

Figure 1 shows a meridional projection of a typical centrifugal compressor stage, where all the major components are labeled for a quick reference.

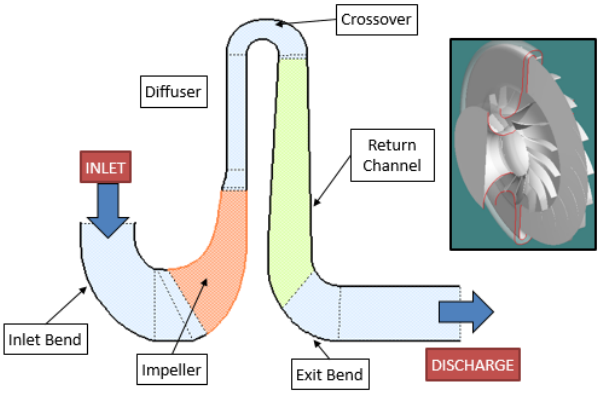

Figure 1. Typical Medium-to-High Flow Centrifugal Stage

Such a centrifugal stage can be characterized by well-known non-dimensional parameters as given below:

$$\text{Flow Coefficient, } \varphi = \frac{Q_0}{\pi \cdot r_2^2 \cdot U_2} \quad (1)$$

$$\text{Head Coefficient, } \mu = \frac{H_p}{U_2^2} \quad (2)$$

$$\text{Work Coefficient, } \tau = \frac{\Delta h_t}{U_2^2} \quad (3)$$

$$\text{Machine Mach Number, } M_U = \frac{U_2}{a_0} \quad (4)$$

For a fixed tip speed (U_2) and tip diameter (d_2), increase in the inlet volume flow of Q_0, will clearly increase flow coefficient (ϕ). Alternatively, in order to maintain ϕ while increasing Q_0, either d_2 or U_2 or both must increase, which means the machine scales up and/or runs faster, which is acceptable but only up to a certain limit.

Another, perhaps more popular, method of characterizing various turbomachinery is the use of specific speed (N_s) and Specific Diameter (N_d), which are defined as follows.

$$\text{Specific Speed, } N_s = \frac{\omega\sqrt{Q_0}}{H_p^{3/4}} \quad (5)$$

$$\text{Specific Diameter, } D_s = \frac{D_2\sqrt{H_p}}{\sqrt{Q_0}} \quad (6)$$

A number of researchers have explored the relationship of these variables. Casey (2010) reproduced the classic Cordier diagram accompanied by a very insightful discussion on how specific speed and Cordier line indicate the most suitable impeller architecture for the given duty (head coefficient and volume flow rate). The specific speed also determines an important impeller design parameter – impeller inlet to outlet diameter ratio. As seen from Figure 2, as the specific speed increases, the impeller style changes from a purely radial discharge to a mixed and finally purely axial flow. The Cordier line shows some of the best available turbomachines for that given specific speed regardless geometric similarities.

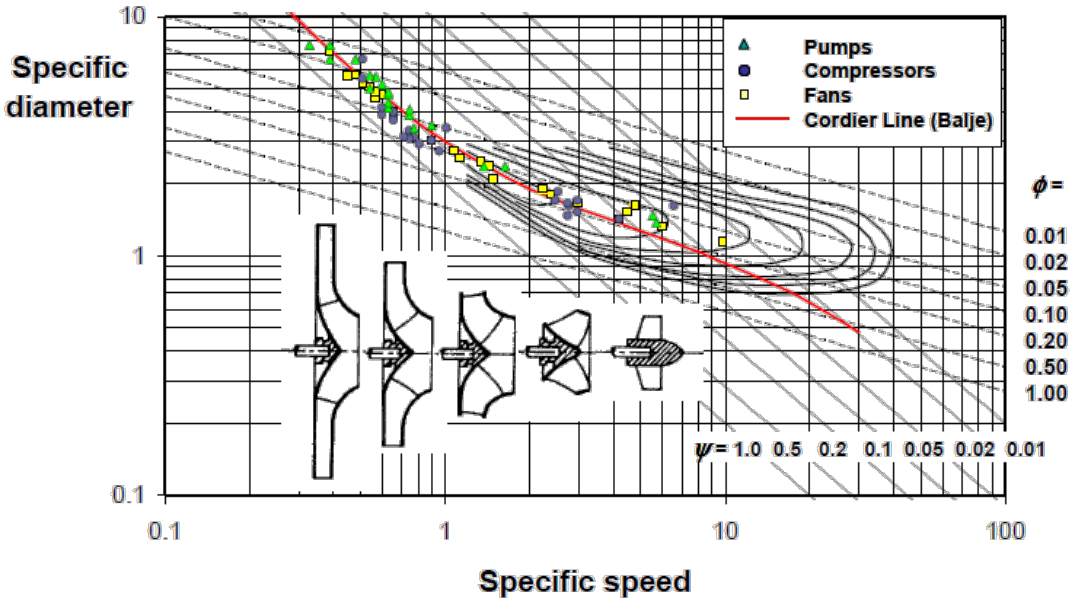

Figure 2. Specific Speed and Specific Diameter from (Casey, 2010)

The very high flow (VHF) design described in this paper enhances the pre-existing impeller lineup by approximately 32% in terms of flow capacity. The nominal design flow coefficient was set at 0.24. Specific speed and specific diameter are 1.55 and 1.91, respectively. This indicates that optimum design would be of a mixed flow style impeller. Over a range of specific speeds, both styles of impellers can overlap and final choice will depend upon the details of the design and performance expectations. The Machine Mach Number (M_U) for the chosen design targets is 0.88.

Figure 2 further shows that purely radial centrifugal stages with the best efficiencies have a nominal head coefficient (denoted by ψ) of 0.55, which also is a good target for this VHF design. Albeit from the same figure, achieving such a head coefficient level would place the design (with a specific speed of 1.55) far from the Cordier line. This indicates that chosen design targets make it challenging to achieve peak performance.

The stage (performance) map width is one of the harder design targets to achieve in this flow regime; and it is impacted significantly by the details of the design – specifically impeller design. The compressor characteristics also have certain shape targets for example, *% Head Rise to Surge (%HRTS)* and *Turndown*, in conjunction with the targeted map widths. These off-design performance expectations make this further challenging due to rapid performance deterioration caused by increased sensitivity to incidence mismatch, and other loss mechanisms.

Impeller Design

Generally, the centrifugal stage characteristics are determined by entry and exit blade shapes (Rodgers, 1998) as well as Mach number levels. The head requirements and available speed typically drive the inlet and discharge vector diagrams for most turbomachinery designs.

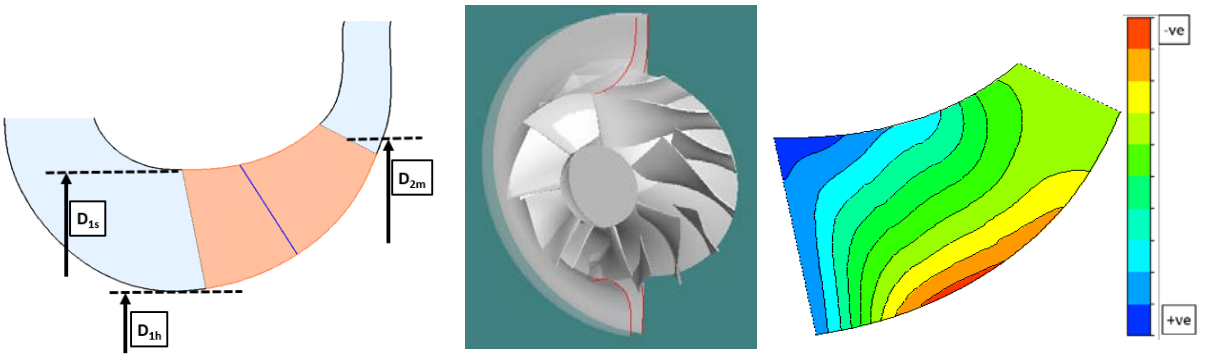

a. Meridional Shape b. 3-D View c. Blade Angle Contours (with respect meridional direction)

Figure 3. VHF Impeller

Figure 3 (a and b) shows the prototype VHF stage with a clear, mixed flow discharge. The general meridional shape and inlet and discharge blade angles as well as number of blades were determined in conjunction with meanline and more detailed CFD analyses. The average tip diameter was maintained similar to the existing impeller lineup. The inlet bend curvatures are generous to reduce shroud meridional velocity at impeller eye. The inlet hub diameter (D_{1h}) was constrained to achieve necessary rotor stiffness, while the impeller eye or shroud inlet diameter (D_{1s}) was selected to minimize the shroud Inlet Relative Mach Number (Ma). Both hub and shroud contour are designed to control curvature and diffusion within the impeller passage. Low levels of sufficiently smooth curvatures are necessary to prevent unintended acceleration as well as flow separations. The longer axial impellers help achieve this but may result in excessively long rotor length. The impeller inlet bend, impeller, and turning of impeller exit to into radial diffuser (vaneless) were successively compacted to control stage space. The impeller hub section is not usually loaded strongly, but it still needs to be controlled for minimizing the curvature.

In this high flow coefficient regime, the inducer design becomes very important. This entry section directly influences both aerodynamic and geometric throat areas, which are linked to maximum flow capacity. The splittered configuration that is seen in Figure 3's 3-D view helps in achieving the geometric throat necessary for the intended choke flow. More importantly, however, the splitter allows control of blade loading inside the impeller passage. This, in turn, reduces the impeller's sensitivity to off-design condition as well as to the deviations in manufacturing and other processes. For the VHF stages, main and splitter blades were constructed largely independent of each other. Figure 3a shows the splitter LE position (blue line), which was iteratively determined to balance the blade loading for the required flow range. Circumferentially, the splitter was located closer to main blade suction surface. This helps in managing passage aerodynamic blockage development, which in turn promotes circumferentially more uniform impeller discharge flow profiles.

At design point, the Inlet Relative Mach Number (Ma) is in the high subsonic region (≈0.9) near the critical shroud section. This also points at the possibility of shock and associated losses especially at higher than design speed. Transonic blading is beneficial to control the acceleration of the fluid over the blade suction surface that could lead to shock. Also, the shock-boundary interaction (and associated losses), and secondary flows within the impeller have to be managed. The leading edge (LE) shape, thickness and blade turning (blade angle (β) distribution) have been carefully selected using CFD analyses to reduce these loss-causing mechanisms.

As seen in Figure 3c, the blade angle (β) contours near shroud for the transonic inducer is characterized by very little turning to reduce loading and thus, sensitivity to incoming flow conditions. This actually causes the throat area to be reduced. In the case of a high Mach number impeller, however, this same blading can reduce shock losses and blockage accumulation up to the throat resulting in higher than anticipated choke flow (Rodgers, 1998).

In the present VHF design, a custom bowed blading profile provides a controlled degree of tangential sweep primarily for hub to shroud loading management. Such bowed blading in conjunction with hub and shroud β distributions control the local blade loadings thereby maximizing performance at design condition while still maintaining strong aerodynamic performance at off-design conditions.

The impeller exit width to tip diameter (b_2/D_2) is an important parameter, which is determined based on the head requirements. The shape of the impeller blade tip has been chosen to produce uniform flow exiting the impeller, which can strongly affect the performance of the downstream stationary components and stall-side range.

Stationary Component Design

The stationary components design efforts were nearly as extensive as those for the impeller. Figure 4 shows the meridional view of the entire prototype VHF stage. The diffuser for the VHF begins with a curved inlet, which is rapidly turned into the conventional parallel-walled radial diffuser with pinch levels that were iteratively refined. The diffusion-controlled crossover passage is shaped to minimize the accumulation of low-momentum fluid and to eliminate reverse flow in the crossover shroud region at design and near design flow conditions.

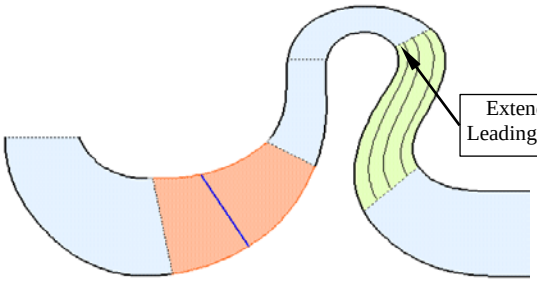

Figure 4. VHF Stage Meridional Projection

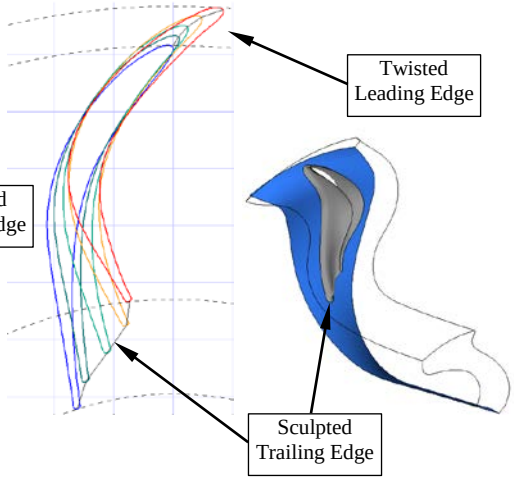

Figure 5. Extended Sculpted Return Channel Vanes

The further advancement in the stationary performance comes from the return channel design for this stage. The return channel houses fully 3-D vanes as opposed to traditional 2-D vanes. This can be clearly seen in Figure 5. To reduce the deleterious aero-mechanical interaction with the downstream stage, the number of vanes for this VHF stage was kept low at around 12 vanes. The iterative design process resulted in vanes featuring a twisted leading edge extending into the crossover, and highly sculpted trailing edge to provide a near-uniform distribution of swirl exiting the flow profile (Jariwala et al., 2016, and US Patent Application US20180347584A1).

In summary, the present VHF stages include a host of advanced features. The covered impeller has splittered configuration with transonic-style inducer, fully 3-D sculpted blades with custom hub-to-shroud thickness distribution, and a highly optimized tip shape to provide uniform flow to a curved diffuser. The diffuser rapidly turns into a conventional parallel-walled diffuser to save axial stage space. The diffusion-controlled crossover transmits the flow into a return channel with fully 3-D vanes that produce near-uniform swirl with low total pressure losses.

Design Analysis

A single-sector, steady 3D RANS CFD model (Figure 6) was used during the aerodynamic design cycle. The computational domain included a short inlet bend, an impeller, a vane-less diffuser, and a single-vane passage return system. Fillets were included as part of the geometry, while the secondary flow passages (seals) were excluded from the computational domain. The component surface roughness was also included. Structured meshes were comprised of approximately 3.2 million total nodes.

Based on past practice, this level of mesh resolution was judged to be acceptable for resolving the principal aerodynamic mechanisms linked to quality design choices, at least on a relative basis.

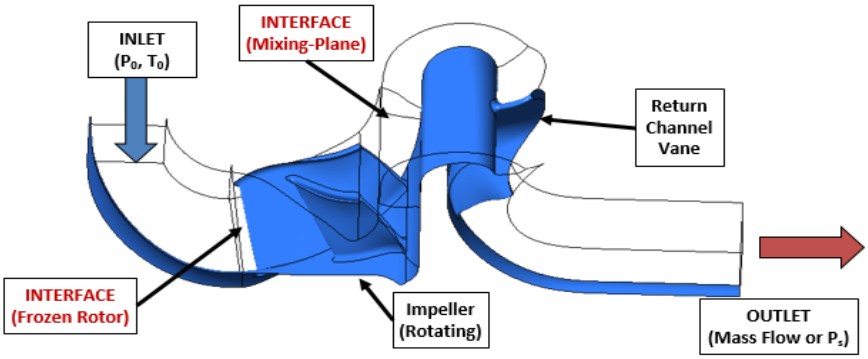

Figure 6. CFD Domain for Design Cycle Analysis

To understand the quality of CFD-predicted flow fields, the VHF stage has been compared with the well-proven previous high flow stage (design $\phi \approx 0.18$). Both cases were run at their respective design flow coefficient but at the same Machine Mach Number (M_U = 0.88). If the new stage shows similar or improved flow field quality, it would indicate strong basis in the proven design.

Figure 7 shows the Inlet Relative Mach Number (Ma) contours in the B2B plane at the 95% span. The VHF stage shows similar quality and levels as the previous high flow stage, indicating the flow quality has been maintained. The inducer section of the VHF stage has cleaner flow, which is important for achieving flow range. The low momentum fluid in the splittered section in the exducer region is thought to have originated from migration of low momentum fluid from hub toward shroud under centrifugal effect.

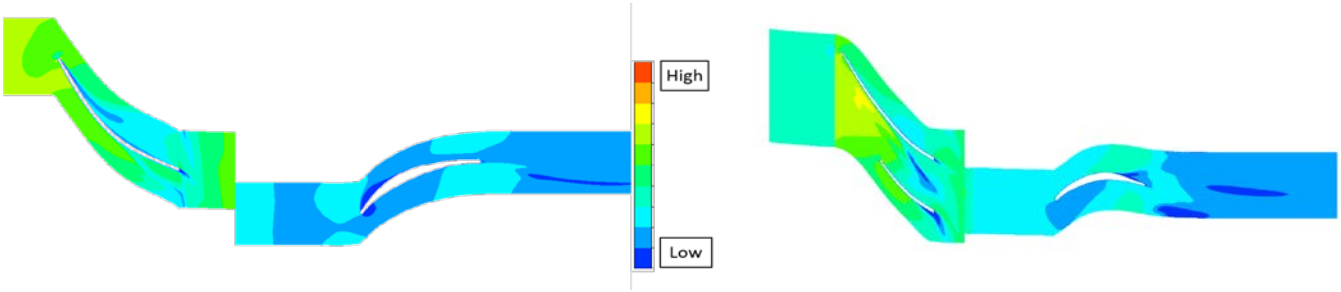

Previous High Flow Stage (Design ϕ=0.18) VHF Stage (Design ϕ=0.24)

Figure 7. Relative Mach number Contours at 95% Span in B2B Plane, One Impeller Sector Shown

Figure 9 shows the circumferentially mass-averaged Ma in stationary frame, and meridional velocity (V_m) contours at design flow and Mu=0.88. The left column shows the HF stage, and the right column shows the VHF stage. VHF stage Ma contours are well-distributed without any unintended accelerations or low-momentum flow, except for a slight Mach number increase in the exducer (near discharge) section, where the HF stage has worse accelerations. In the diffuser, we see a more uniformly distributed gradient for the VHF stage compared to the HF stage. On the V_m contours, the VHF stage has much better distribution of the gradient throughout the stage. The diffuser of the VHF stage has significantly cleaner flow. The VHF stage has a relatively longer axial length impeller, which is coupled with a generous inlet bend to reduce the inlet distortion. Together, this increases the stage space to some extent, but the overall machine size still reduces as will be shown later.

Previous High Flow Stage (Design ϕ=0.18) VHF Stage (Design ϕ=0.24)

Figure 8. Mach Number (Ma) in Stationary Frame Comparison at Design Flow (Mu=0.88)

Previous High Flow Stage (Design ϕ=0.18) VHF Stage (Design ϕ=0.24)

Figure 9. Circumferentially Mass-Averaged Meridional Velocity (V_m) Comparison at Design Flow (Mu=0.88)

The comparison of polytropic head and efficiency are shown in Figure 10 between these two stages. The efficiency of the VHF stage is higher over the entire range, while the operating range has also improved on a relative basis. In addition, the curve shapes and map widths are very comparable. This indicates the technological advancement achieved by this VHF stage.

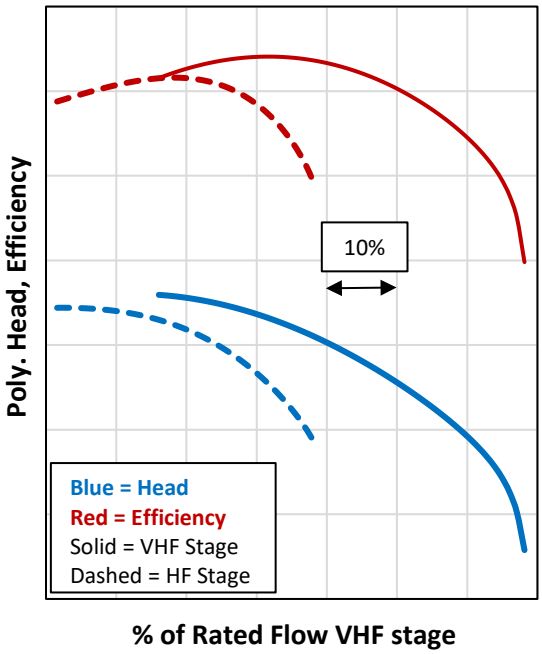

Figure 10. Comparison of Stage Performances at Mu=0.88

Solid Mechanics (structural)

Mechanical qualification of high flow impellers for high-speed applications without compromising the aero performance poses a significant challenge. As shown in the previous section, while a thin leading edge blade and 3-D features such as twisting and sculpting improve the aerodynamic performance, they can also create significant structural challenges with respect to limiting the stresses and displacements. Thin blades lead to higher stresses and lower leading edge natural frequencies. Twisted blades tend to *untwist* at speed thereby creating additional bending stress at blade roots thus lowering the allowable spin speed. The design must meet requirements with respect to strain, deflections at critical locations, torque carrying capacity at maximum continuous speed, and resonance margins with respect to excitation frequencies.

Per API 617 8th edition (2014), all impellers must be over-speed tested to no less than 115% of maximum continuous speed. This is usually accomplished in a spin pit. The allowable spin speed is usually determined by using a linear elastic Finite Element Analysis (FEA). In this case, the spin speed limit is determined based on the minimum yield strength of the material.

Figure 11 shows, from left-to-right, the one-seventh sector cyclic symmetry FEA model, solid model, and test impeller. Finite element analysis was conducted using the cyclic symmetry method to qualify the design for spin speeds, frequency and torque carrying capacity.

Figure 11. FEA, Solid Model and Test Impeller

It is important to avoid all of the impeller's excitable modes in the compressor operating speed range. The thin 3-D varying blade designs create lower leading edge natural frequencies. Many design iterations were performed involving both aerodynamic and solid mechanics disciplines for an optimal compromise. The final blade thickness distribution was sufficiently thick to improve the natural

frequencies to achieve the targeted speeds of operation while being sufficiently thin for aerodynamic performance. Figure 12 shows the leading edge and nodal diameter modes for the VHF impeller.

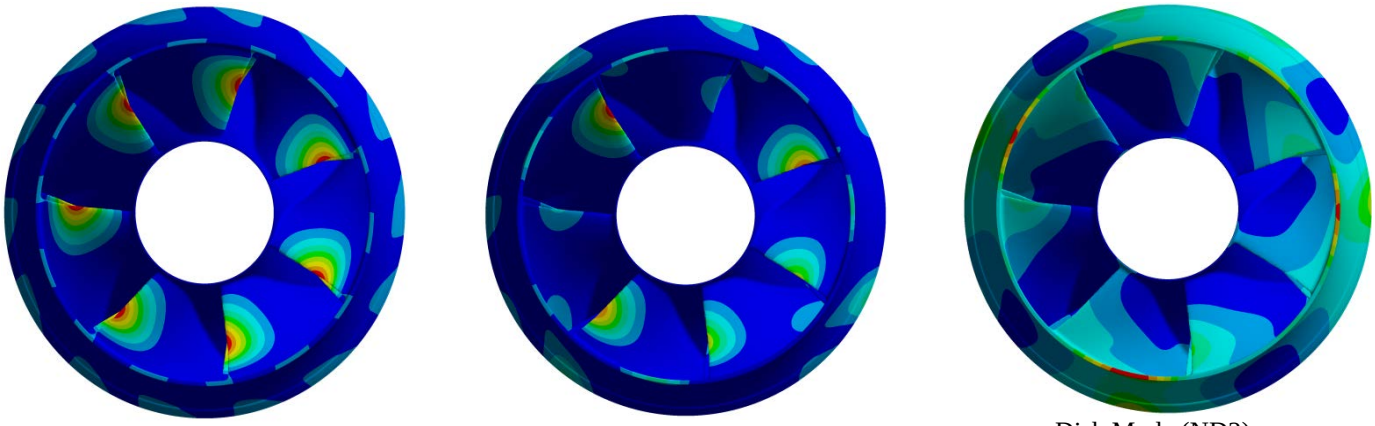

Blade Leading Edge Mode (LE0) Blade Leading Edge Mode (LE2) Disk Mode (ND2)

Figure 12. Impeller Leading Edge and Nodal Diameter Modes (Red and Blue indicate +ve and –ve stresses, respectively)

When selected, impeller stages will have sufficient margin with respect to the following resonance conditions as discussed by Pettinato et al. (2012) and Kushner et al. (2013):

- Disk Critical Speeds
- Leading Edge Impeller Blade Resonance
- Disk Interaction Resonance

Disk Critical Speeds
Disk critical speeds for the reselected first stage and second stage impellers are examined. At a disk critical speed, the relative amplitude of the disk around the circumference in stationary coordinates would form a standing wave in stationary space. The modes of concern are up to the number of rotating impeller blades divided by two.

Leading Edge Impeller Blade Resonance
Blade resonance for the impeller blade's leading edge is a concern especially for impellers having a full inducer such as this VHF design. The blades were designed to have high leading edge natural frequency to ensure high speed application. However, some limitations may occur when paired up with a high number of upstream return channel vanes.

Disk Interaction Resonance
Besides disk critical speeds, there also can be excitation at harmonics of speed, especially from upstream and downstream vanes. Kushner (1980) developed a set of parametric equations for evaluating interaction resonance using the number of rotating blades to determine the excitation and response potential. For certain combinations of the two numbers, the coupled blade/disk modes with diametric nodal lines are either phase cancelled or excitable when an excitation source coincides with a resonant mode. These equations are represented as follows:

When not at a disk critical speed,

$$|y \cdot S| \pm |z \cdot B| = n \quad (7)$$

$$y \cdot S = h \quad (8)$$

$$f_r = y \cdot S \cdot \omega \quad (9)$$

Whereas when at a disk critical speed, for B > 1

$$y \cdot S = h = n \quad (10)$$

$$f_r = n \cdot \omega \quad (11)$$

where:

B = Number of rotating blades
S = Number of stationary elements

f_r = Natural frequency at speed, Hz
h = Harmonic of speed
n = Number of diameter nodal lines
y & z = Integers > 0
ω = Rotating speed, Hz

The takeaway from these equations is that interaction resonance requires *both* operation on top of a resonant speed and a combination of vanes and blades that will produce an excitation pattern that coincides with the mode shape. One effective way to avoid significant minor interaction resonance is to have a difference of one (1) between the stationary vanes and rotating blades. The 1-diameter mode couples to the shaft and is extremely difficult to excite.

Rig Performance Testing

The VHF stage was designed at the same scale as that of the test configuration to directly compare test results with the estimated performance. Notably, the impeller was manufactured as a single-piece component. The sculpted 3-D return channel vanes were manufactured using 5-axis milling process. Figure 13 shows the impeller and stationary components.

VHF Impeller Stationary Components

Figure 13. VHF Impeller and Stationary Components

The schematic of the test facility is shown in Figure 14. It is a closed loop system with Nitrogen or R-134A as available test gases. The test article is driven by an electric motor through a speed-increasing gearbox. The assembly arrangement of the test article is modular in nature, with different components stacked axially around a shaft. The impeller has an axial inlet and radial discharge. The inlet plenum upstream of the test impeller can be configured with either first-stage or intermediate-stage style inlets.

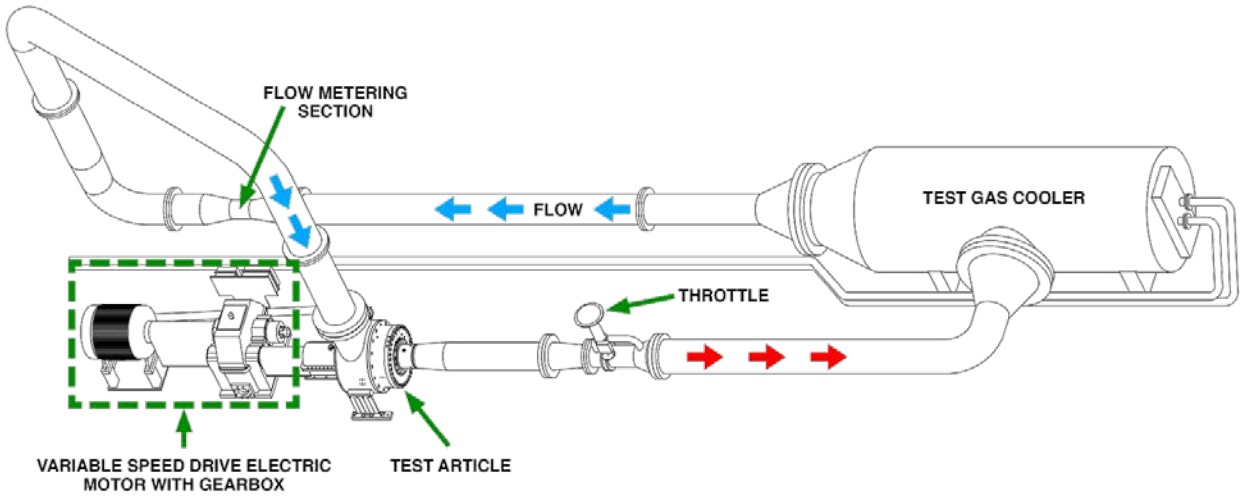

Figure 14. Test Facility Schematic

Figure 15 shows the test layout for the prototype VHF stage. The inlet plenum routes the incoming flow through stationary guide vanes into the impeller. The critical stations are instrumented as shown in Figure 15. The impeller exit (STA-2) proved to be hard to access for the traverse probe. Instead, two circumferentially spaced Kiel rakes, each with 5 Kiel probes, were provided. This was also the case for the crossover exit (STA-6). At these locations, the static pressure taps were provided on both hub and shroud to complete the pressure profiles. The diffuser exit (STA-4) and stage exit (STA-7) were instrumented with 3-hole Cobra traverse probes that provided spanwise velocity profiles. STA-7 additionally had total pressure and total temperature probes as well. Several speed-lines (mostly using R-134A) were run to characterize the stage performance map. The swirl exiting the stages was measured at various operating points. The dynamic probes installed in the diffuser hub wall were used for rotating stall measurements.

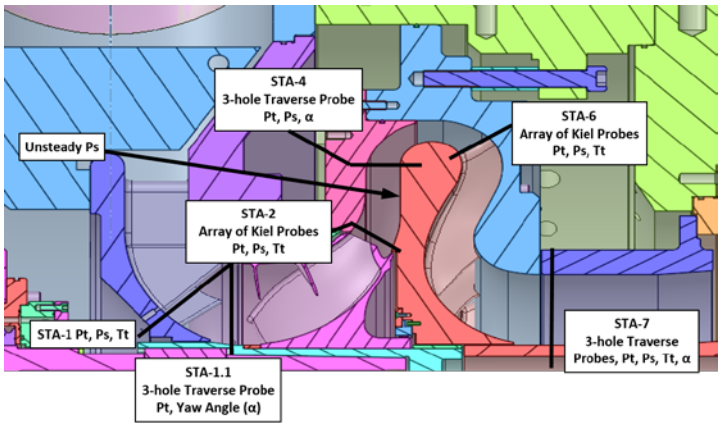

Figure 15. Test Layout and Instrumentation for VHF Stage.

Results

Figure 16 shows the air equivalent (P_0 = 1 bara, T_0=27 C) tested performance in terms of polytropic head and polytropic efficiency, respectively. The curve shapes generally appear healthy, and do not display any undesirable elements like head droop. For the speeds higher than the design speed, stonewall characteristics are well defined with rapid drop in head. At the Mu of 1.14, the performance degrades rapidly, which is evident by lower peak polytropic efficiency levels in Figure 21. Notably, the peak efficiency of the prototype VHF stage occurs at a flow coefficient lower than the design. This could be attributed to aerodynamic mismatching of the components resulting from manufacturing, assembly and other variances due to tolerance stack up. This also indicates the value of a rig test to account for real-life differences between predictions and actual performance. For the final implementation of the family, a stage meeting original target flow coefficient was created through flow extension.

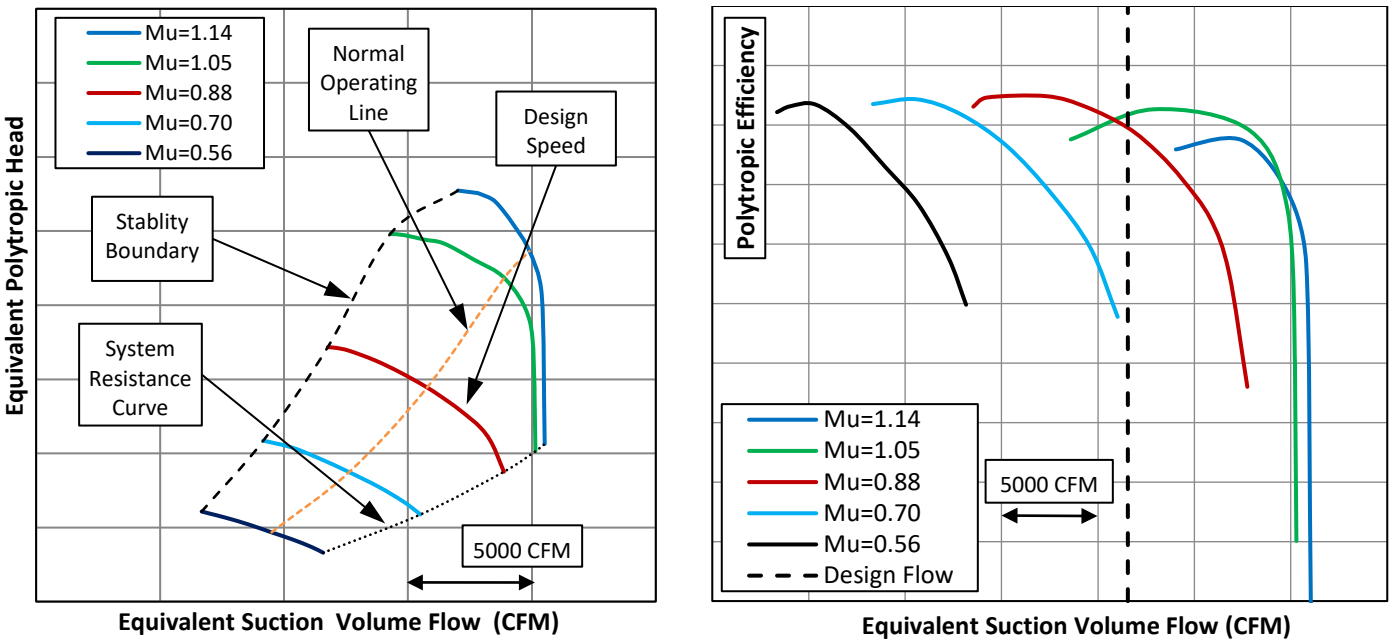

Polytropic Head vs. Flow Polytropic Efficiency vs. Flow

Figure 16. VHF Stage Performance Map

The performance map width for the new stage is very respectable and sufficiently wide. As shown in Figure 17, the important % Head Rise to Surge (%HRTS) and stable operating range are better than the previous high flow stage on relative basis.

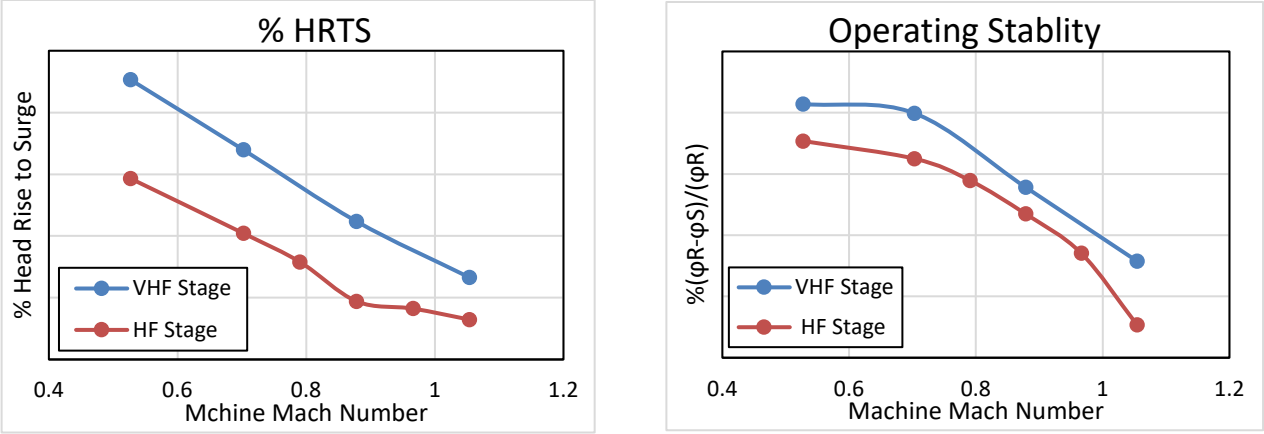

Figure 17. VHF and HF Stage Map Characteristics

PRACTICAL APPLICATION AND CASE STUDIES:

An example application is presented where an already operational compressor has been reselected, taking advantage of the available VHF family of stages. This is followed by discussion of two recent shop orders that utilize the new VHF stage family. These two shop orders were successfully performance tested and are expected to enter service mid-2020. One set of performance test results is provided.

110M Compressor Reselection to 103M Compressor Using VHF Stages

Figure 18 shows a 110M frame size booster compressor that has been operating in the field since 2011 compressing a mixed hydrocarbon gas. It is a straight through 6-stage machine. The 110M is the largest frame size that the OEM offers. The scale of this frame can be understood by comparing the impeller size with reference to an average-sized person standing next to it with a smaller scale impeller. The impeller diameter was 1.93 m. The weight of this machine was 232,000 kgf. The first stage has the highest flow coefficient (0.16), whereas the final stage has the lowest flow coefficient (0.039).

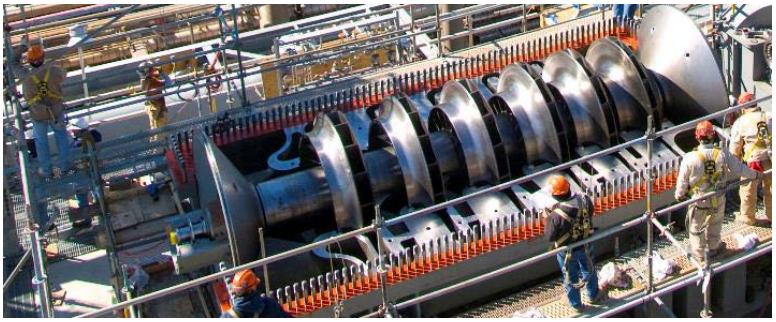

Figure 18. 110M Product Booster Compressor in Field (Case-1)

A first pass reselection of this compressor using the latest VHF stages results in a full frame size reduction to 103M having 7-stages. The first stage of this reselection would be a VHF stage that would push the flow coefficient slightly beyond the design coefficient of the highest available stage up to 0.27. The second stage would also be a VHF stage having a flow coefficient of 0.21. The smallest flow coefficient would occur at the last stage having a flow coefficient of 0.050. The wheel diameters are reduced from 1.93m to roughly 1.65m while the weight is reduced by more than 45,000 kgf (21%). Table 1 provides additional comparisons. The effect of the frame size reduction that is made possible by the new VHF stages can be easily seen and appreciated. In addition to the size reduction, the machine speed would increase from 2787 RPM to 3010 RPM at design speed, and 2926 RPM to 3160 RPM at maximum continuous speed.

Table 1. Benefits of New VHF Stage Family (Reselection example going from HF to VHF).

Case	Service	Selection	Frame Size	# of Stages	Compressor Weight		Bearing Span		Highest Design ϕ
					(kgf)	(lbf)	(m)	(in)	(dim)
1	Product Booster	HF Original	110M	6	232000	512000	6.39	251	0.16
		VHF Reselect	103M	7	184000	406000	7.18	283	0.25
		Δ	-1	+1	-21%		+12%		+57%

Reselection Disk Critical Speeds

Disk critical speeds for the reselected first stage are examined. The resonant frequency versus nodal diameters is shown in Figure 19. Large margins from disk critical speeds are present for this VHF stage.

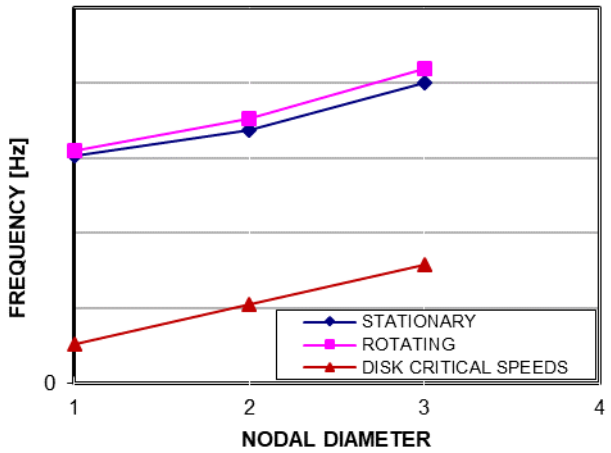

Figure 19. Impeller Disk Critical Speeds

Reselection Blade Leading Edge Resonance

The leading edge blade resonance for the reselected first and second stage impellers are examined. An impeller blade's leading edge natural frequency is a concern especially for impellers having a full inducer, which both VHF impellers have. Figure 20 shows the Campbell Diagrams for the first leading edge blade modes. The separation margin was acceptable.

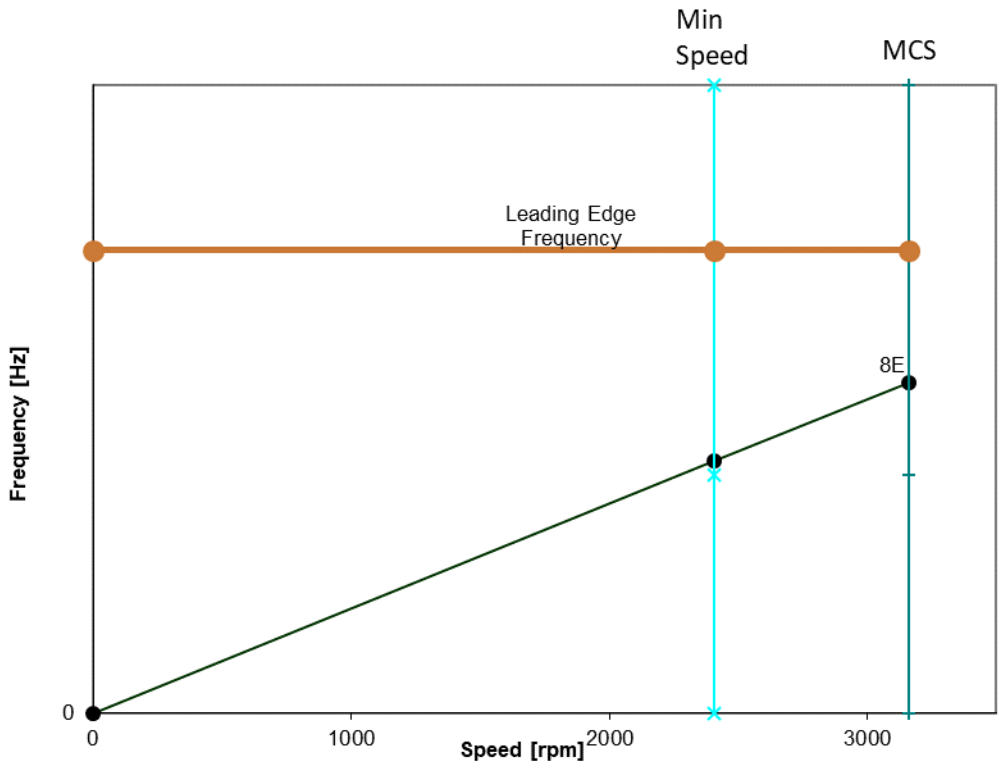

Figure 20. 1st Stage Impeller Campbell Diagram of the Blade Leading Edge Mode

Reselection Minor Interaction Resonance
The VHF stage with seven full blades is paired with an eight per rev inlet section. The difference is one. One diameter modes tend to couple to the shaft and are therefore not a concern. The diffuser is vaneless and thereby does not provide any interaction excitation.

VHF Compressor Reselections Reverting to HF Technology
Table 2 lists two shop orders that have been completed and shipped with the VHF stage families. Just for comparison purposes, they have been reselected without the use of VHF stages, and listed under "HF Reselect". Again, the benefits of having the effect of the frame size reduction that is made possible by the new VHF stages are easily seen. The VHF stages result in a 23% and a 24% weight reduction, respectively.

Table 2. Benefits of New VHF Stage Family (Reselection example going from VHF to HF).

Case	Service	Selection	Frame Size	# of Stages	Compressor Weight		Bearing Span		Highest Design ϕ
					(kgf)	(lbf)	(m)	(in)	(dim)
2	Wet Gas Compressor	HF Reselect	56MB	6	63000	139000	3.26	128	0.16
		VHF Original	46MB	6	49000	107000	3.15	124	0.25
		Δ	-1	0	-23%		-3%		+34%
3	Butane Compressor	HF Reselect	70MB	5	98000	216000	3.48	137	0.19
		VHF Original	60MB	5	75000	165000	3.38	133	0.25
		Δ	-1	0	-24%		-3%		+27%

Shop Order Results:
Figure 21 shows performance test results from a recent shop order. The solid model shows the first stage from the VHF family. The tested performance compared very well with the predicted performance.

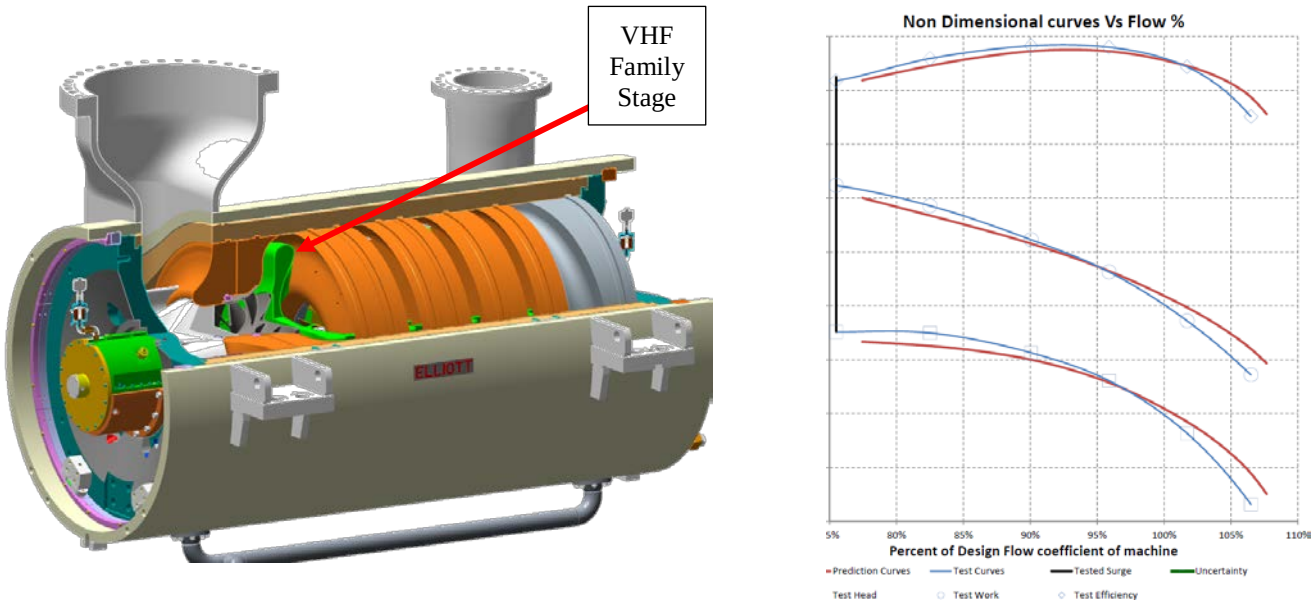

Figure 21 Shop Test Results (2019)

CONCLUSION

This paper discussed the development of a very high flow coefficient stage having a flow coefficient of 0.24 and leading to a creation of stages covering design flow coefficients from 0.18 to over 0.25. These high flow coefficient stages include the following features:

- Splittered blade design with 7-full and 7-partial blades.
- Inducer section that includes some transonic features
- Mixed-flow exducer
- Customized impeller blade tip shape
- Hub-to-shroud blade tapering to improve frequency margins
- Fully 3-D return channel vanes to provide low total pressure drop and more uniform distribution of swirl

The stage was rig tested and met the efficiency target and demonstrated usable range and head. A reselection exercise of an in-service machine as well as further examination of two actual compressor shop orders with VHF stages detail the benefits of this new impeller line-up. In all cases, the frame size reduced, supporting the objective of lowering the equipment cost. The reduction in frame size not only has up-front cost benefit, but also life-cycle and operational cost benefits. The strong agreement between recent shop order tests and predictions have bolstered the confidence in the new VHF stages' ability to help create cost-effective compression equipment.

ACKNOWLEDGEMENT

The authors would like to thank Elliott Group management for granting us permission to publish this work. Elliott Core Application Engineering has been a great help with respect to compressor applications aspects of this work.

NOMENCLATURE

A	Passage Area [m^2]
b	Passage Height [m]
m	Meridional Coordinate [m]
Ma	Inlet Relative Mach Number
Mu or M_U	Machine Mach Number
Ps	Static Pressure [bar]
t_b	Blade Thickness [inch]
Pt	Total Pressure [bar]
R	Radius [m]
STA	Station
V	Total Velocity [m/s]
V_m	Meridional Velocity [m/s]
V_θ	Tangential Velocity [m/s]

α	Swirl Angle, $\alpha = \tan^{-1}\left(\frac{V_\theta}{V_m}\right)$ [°]
β	Blade Angle Referenced from Meridional Direction [°]
φ	Flow Coefficient
τ	Work Input
μ or ψ	Head Coefficient
η	Efficiency
ρ	Density [kg/m^3]

Subscripts

0	Inlet Station
2	Impeller Exit Station
4	Diffuser Exit Station
6	Crossover Exit Station (Upstream of Vane Leading Edge)
7	Vane Trailing Edge Station
8	Return Channel Exit Bend Discharge Station
s	Static
t	Total
x	Station

REFERENCES

API 617, 2014, "Axial and Centrifugal Compressors and Expander-compressors", Eighth Edition, American Petroleum Institute, Washington, D.C.

Anon., "A mega compressor in Houston," Turbomachinery International, July/August, 2009.

Aungier, R. H., "Centrifugal Compressors – A Strategy for Aerodynamic Design and Analysis", The American Society of Mechanical Engineers, New York (2000) ISBN: 0791800938

Casey, Michael, Zwyssig, Christof, and Robinson, Chris. "The Cordier Line for Mixed Flow Compressors." Proceedings of the ASME Turbo Expo 2010: Power for Land, Sea, and Air. Volume 7: Turbomachinery, Parts A, B, and C. Glasgow, UK. June 14–18, 2010. pp. 1859-1869. ASME. https://doi.org/10.1115/GT2010-22549

Corbo, Simone; Guglielmo, Alberto; Valente, Roberto; Iurisci, Giuseppe (2018). New Challenges and Design for High Mach High Flow Coefficient Impeller for Large Size LNG Plant. Turbomachinery Laboratory, Texas A&M Engineering Experiment Station. Available electronically from http://hdl.handle.net/1969.1/175000

Harvey, Shane. "Balancing the Economies of Scale", Hydrocarbon Engineering, July 2019.

Kushner, F., 1980, "Disc Vibration — Rotating Blade and Stationary Vane Interaction," ASME Journal of Mechanical Design, 102, pp. 579-584. https://doi.org/10.1115/1.3254788

Kushner, F., Strickland, R. A., and Shurina, J., 2013, "Rotating Component Modal Analysis and Resonance Avoidance – An Update," Tutorial, Proceedings of the 42nd Turbomachinery Symposium, Turbomachinery Laboratory, Texas A&M University, College Station, TX. https://doi.org/10.21423/R1TP91.

Jariwala, Vishal, Larosiliere, Louis, and Hardin, James. "Design Exploration of a Return Channel for Multistage Centrifugal Compressors." Proceedings of the ASME Turbo Expo 2016: Turbomachinery Technical Conference and Exposition. Volume 2D: Turbomachinery. Seoul, South Korea. June 13–17, 2016. V02DT42A032. ASME. https://doi.org/10.1115/GT2016-57777

Louis M. Larosiliere, Vishal Jariwala. "Extended Sculpted Twisted Return Channel Vane Arrangement," US Patent Application: US20180347584A1 (2017)

Ludtke, K. H., "Process Centrifugal Compressors: Basics, Function, Operations, Design, Application", Springer-Verlag Berlin Heidelberg (2004) ISBN: 3540404279

Pettinato, B. C., Griffin, J. H., Wang, Y., Feiner, D. M., Echols, B., and Cushman, M., 2012, "Experimentally Based Statistical Forced Response Analysis for Purpose of Impeller Mistuning Identification," Proceedings of the Second Middle East Turbomachinery

Symposium, Turbomachinery Laboratory, Texas A&M University, College Station, TX. http://hdl.handle.net/1969.1/172623

Rodgers, C. "The Centrifugal Compressor Inducer." Proceedings of the ASME 1998 International Gas Turbine and Aeroengine Congress and Exhibition. Volume 1: Turbomachinery. Stockholm, Sweden. June 2–5, 1998. V001T01A009. ASME. https://doi.org/10.1115/98-GT-032

Ronald Josefczyk and Daniel Jones, “Design Challenges to Apply Mixed Flow Impeller Technology to 3000 Kta Ethane Cracker”, 30th 2018 AIChE Spring Meeting and 14th Global Congress on Process Safety, Paper #33D.

